DNA CHARGE TAGS AS ELECTRONIC LABELS FOR DNA MICROCHIP TESTING

Victor W. Weedn, MD, JD,
David M. Sipe, PhD, Alan Rosenbloom, MD
Carnegie Mellon University

ABSTRACT

Project Goals and Objectives: We proposed to develop electronic labels, "charge tags", analogous to fluorescent labels for use in the detection of DNA Short Tandem Repeat (STR) fragments for use on microchips.

Proposed Research Design and Methodology: Large dipole moments can be suddenly created from hybridization of a probe and target where charges of opposing sign are placed on opposing ends of the target and the probe. We intended to detect the presence of these dipoles using Dielectric Relaxation Spectroscopy (DRS). DRS is a method to analyze polarized molecules through AC impedance changes during high frequency sweeps. We had hoped that by specifically engineering dipoles and creating sudden and large dipole shifts that we could generate a specific signal and further that this signal would relate to the dipole length—thus differentiating STR repeat fragment length sizes. Thus, we had intended to create a revolutionary new technique which would be faster (because it would not require electrophoretic separation) and cheaper (because it would not require expensive fluorescent dye reagents). Furthermore, we may have been able to create potentially inexpensive, possibly disposable, integrated microchip platforms to employ such systems.

Results: Although we were able to generate DRS signals from certain small molecules, we were unsuccessful in obtaining a signal using DNA fragments. Significant salt concentrations were necessary to keep such high concentrations of DNA in solution. Salts create a very large dipole signal that we believed effectively masked the signal that we were attempting to detect. Had we been able to detect a signal, we had hoped to greatly improve the sensitivity of the system through optimization of the instrumentation involved.

CHARGE TAGS AS ELECTRONIC LABELS FOR DNA MICROCHIP TESTING

Victor W. Weedn, MD, JD,
David M. Sipe, PhD, Alan Rosenbloom, MD
Carnegie Mellon University

We explored the use of electronic labels, "charge tags", analogous to fluorescent labels, for the detection of DNA Short Tandem Repeat (STR) fragments for use on microchips.

Large dipole moments can be suddenly created from hybridization of a probe and target where charges of opposing sign are placed on opposing ends of the target and the probe. We explored the use of Dielectric Relaxation Spectroscopy (DRS) to detect such dipoles. DRS is a method to analyze polarized molecules through AC impedance changes during high frequency sweeps. However; the use of DRS in biological systems is limited by fundamental issues such as high conductivity of physiologic solutions and spectral blurring due to complex charge geometry. In fact, very little investigation of this arcane technique has been conducted to date. We had hoped that by specifically engineering dipoles and creating sudden and large dipole shifts that we could generate a specific signal and further that this signal would relate to the dipole length—thus differentiating STR repeat fragment length sizes. If successful, DRS would be a revolutionary new technique which would be faster (because it would not require electrophoretic separation) and potentially cheaper (because it would not require expensive fluorescent dye reagents). Such technology might have eventuated in inexpensive, disposable and fieldable DNA detection chips.

This project proceeded more slowly than anticipated for various reasons. The project required specialized electronic equipment that operates at frequencies into the microwave region. Sample chambers and electrode arrays had to be specifically designed and fabricated. The DRS literature is sparse and conflicting with respect to large biomolecules. This involved ion-beam work at the Penn State and Cornell nanofabrication centers. We achieved replication of typical DRS spectra and were able to establish certain parameters and understandings for the types of analytes we are interested in. However, traditional DRS is an insensitive technique, requiring high concentrations of analytes. To keep the analytes in solution requires high salt concentrations that we believe masked the relevant DRS DNA signal. Thus, we were unsuccessful in demonstrating proof of concept.

BACKGROUND

The forensic DNA community has witnessed a significant evolution in DNA typing technology, yet the desire of even better technology persists. This project was pursued with this quest for better, cheaper, faster DNA testing in mind. The investigators are of the opinion that microchip technology holds promise to accomplish such a goal. However, most DNA microchip strategies attempt to miniaturize traditional DNA typing

techniques; i.e. capillary electrophoresis (Dan Ehrlich, Whitehead Institute), PCR (Allen Northrup, Cepheid), and hybridization (Ron Sosnowski, Nanogen). These approaches profit from miniaturization, but do not truly take advantage of fundamental microscale properties. Several groups have considered pure electronic detection systems. Some involve the use of ruthenium-enhanced conductance to distinguish double-stranded versus single-stranded DNA, but they suffer from drawbacks in sensitivity. Motorola has created a system involving conductance through an attached conductor contacting a nearby molecular wire.

We investigated electronic labels, "charge tags," for detection by dipole resonance for use in microchip systems. Specifically, we investigated Dielectric Relaxation Spectroscopy (DRS) to detect and characterize biologic macromolecules as an in-solution hybridization assay. We proposed to use electronic labels ("charge tags") to create a significant DRS signal. By sweeping AC frequency through our interdigitated electrodes we can detect "relaxation" of charged dipoles by simple impedance. We envisioned use of chemical moieties with strong electrical charges (e.g., lysines [K] as positive charges, glutamates [E] as negative charges) as "charge tags" on the ends of the molecules to create strong dipoles. Although DNA has negative phosphate charges along sugar-phosphate backbone, these charges would not have an appreciable effect on the overall dipole moment, unlike a concentration of charges on the end.

We hypothesized that these charge tags could be used to perform forensic DNA identity testing with either fragment length analysis or sequence polymorphism analysis. Conventional forensic DNA testing is based upon analysis of short tandem repeats (STRs), which is a fragment length based analysis. Since the average distance between stacked bases is 3.4 Å in B-form DNA and the . Since most STRs are based on a triplicate repeat sequence, each core repeat would mean a significant difference (approximately 49 Debye, assuming single charges [discussed below]). Thus, the theoretic difference in dipole moment for each STR allele is very large and we anticipated would be easily measurable. Single nucleotide polymorphisms (SNPs) would similarly be detected by use of sequence specific oligonucleotide (SSO) probes engineered to be different lengths.

This DRS method builds on the inherent advantages of microscales in which electrostatic forces dominate. Charge separation could be a measure of fragment length and should increase linearly with increasing dipole size. This is in contrast to electrophoresis or mass spectrometry, wherein resolution decreases with fragment size. DRS analysis dispenses with fluorescent dyes, optical sources and detectors used by current DNA testing efforts. CMOS chip fabrication without further processing may permit small, inexpensive and possibly disposable DNA test devices. Thus, we attempted to detect hybridization events using little more than two electrodes and potentially enabling near-instantaneous, inexpensive, and fieldable analysis of STRs and SNPS.

DIELECTRIC RELAXATION SPECTROSCOPY (DRS)

Biomolecules can spin, twist, vibrate, or stretch rhythmically to an oscillating electric field of a specific frequency. The mass of the molecule and the collective charge distribution determines the frequency of rotation. Higher frequencies may cause resonant oscillations of subunits of molecules. A frequency sweep will rotate the molecules at until a point is reached which is sufficiently fast that the molecule can no longer keep up with the alternating field. At that point the molecules will stop rotating and assume random orientations—so-called "dielectric relaxation." This spectral analysis is known as Dielectric Relaxation Spectroscopy (DRS). In general, the greater the mass of the molecule, the more difficulty it has keeping pace with the electric field and the lower its frequency of relaxation. DRS is not new, but has not been widely applied to biologic solutions. New analytic equipment now allows far more precise measurements than previously possible.

Unfortunately, there are problems with the application of DRS as a tool to specifically identify macromolecules. In physiologic solutions, ions, such as sodium and chloride, create large conductive losses. Furthermore, the ions create a sheath around the polar groups of the macromolecules that may mask the desired signal. A second problem is the complexity of dipole geometry in macromolecules. The multiple internal dipoles contribute to the overall dipole of the molecule tend to blur the relaxation spectrum over a large frequency range. We proposed to use DNA hybridization to create such sudden strong dipoles to overcome these complications. Furthermore, we intended such large dipoles that they should relax at much lower frequencies than ions and other small molecules in physiologic solutions. This has not been previously tried to our knowledge.

Relatively little has been published on the application of DRS to biomolecules and to DNA specifically. Existing literature is conflicting with some groups claiming the existence of relaxation signals from DNA and others denying it. Arguably, the most thorough publication on DNA analysis is a 1998 NIST Technical Note. This report states that there are three types of DNA dielectric relaxation: alpha relaxation at about one Hz, delta relaxation at one MHz, and the gamma relaxation at two GHz. We have focused on the gamma relaxation that occurs at microwave frequencies.

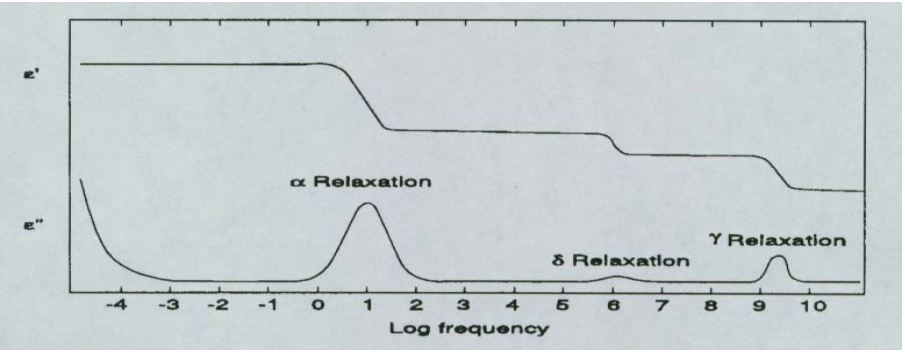

DEBYE DIPOLE MOMENTS

A molecule with a net negative and positive axis forms a dipole. The dipole can be represented as a rod of length *R*, with a charge +*q* at one end and –q at the other end. The separation of charges in space conveys a dipole moment, μ. The Debye (abbreviated as "D") is the unit used to measure the electrical dipole moment. One D = 3.336×10^{-30} coulomb meters (roughly the magnitude of the electric dipole moment of many molecules). The electric dipole moment is a linear function of both the charges and the distance of separation between the charges, so that the dipole moment μ is:

$$\mu = qR$$

When the magnitude is one electronic charge and the separation is one angstrom then the magnitude of the dipole is 4.8 D.

MOLECULAR POLARIZATION

It can be shown that the total molecular polarizability α is:

$$\alpha = \alpha_d + \mu^2/3kT$$

where k is the Boltzmann constant and T is the absolute temperature. α_d is the contribution from distortion factors, the term $\mu^2/3kT$ is the contribution from rotation of the whole molecule. α_d is very small compared to $\mu^2/3kT$. It can be seen from this relationship that the polarizability increases as the *square* of the dipole moment μ. Since μ is proportional to the distance separating the charges of a dipole, this separation has a large effect on the polarizability of a material and hence its dielectric constant.

Also, α is dependent on the frequency of the AC field. At low frequencies, when the entire molecule can rotate, the term $\mu^2/3kT$ dominates. As frequency increases, there comes a point at which the field polarity is changing so fast that the molecular rotations can no longer keep pace with it—the point of dielectric relaxation. At this point, the $\mu^2/3kT$ term approaches zero and α becomes:

$$\alpha = \alpha_d$$

Since α_d gives a very small contribution toward polarizability, the dielectric constant of the bulk material diminishes profoundly at these higher frequencies. This phenomenon is known as dielectric relaxation.

Dielectric Relaxation Spectroscopy (DRS) can be used to characterize macromolecules. The solution containing of the macromolecule serves as a dielectric between two electrodes. The spectrum of dielectric (and hence impedance) changes produced will vary for each macromolecule. The impedance of a capacitor in an alternating current

(AC) circuit is determined by the dielectric constant (*D*) of the material between the plates of the capacitor. The dielectric constant of a material is in turn a measure of its polarizability, i.e., a physical property of the material that allows for the alignment of charges within the material when an AC field is applied to it. The macroscopic polarizability results from the aggregate of contributions of the molecules of the material. The contribution of each individual molecule, denoted α, is due to: 1) alteration of charge distribution within the molecule (i.e. electrons relative to nuclei), 2) re-orientation of the entire molecule in line with its net dipole moment, and 3) displacement of ions within the molecule e.g. proton movement between two carboxyl groups. At low frequencies of alternating current (AC), the re-orientation of whole molecules within the dielectric vastly dominates the other two factors for polar macromolecules such as protein or DNA.

STOKES-EINSTEIN-DEBYE ROTATIONAL CORRELATION TIME

The relationship between the diameter of a biomolecule and its rotation has been described in an equation proposed by Einstein. He hypothesized that charge-based rotational motion of a molecule (rotational diffusion) would be slowed by the frictional forces of a viscous medium. Einstein then combined the dipole moment equation of Debye with the viscosity equation of Stokes to derive the Stokes-Einstein-Debye equation.

If we begin with a population of molecules, all oriented along a single direction, then due to rotational diffusion, the molecules will become less oriented with time. This can be expressed as:

$$\mathbf{W(t) = W(0)e^{-t/t_c}}$$

where W(0) is the net orientation vector at time 0, W(t) is the rotated net vector at time (t), and t_c is the correlation time at which the net orientation of the molecules falls to 1/e of their initial orientation.

Therefore:

$$\mathbf{when\ t = t_c,\ W(t) = 0.37\ of\ W(0)}$$

Taking viscosity into account, and molecular volume, the Stokes-Einstein-Debye equation thus expresses the relationship between molecular rotation and molecular volume, and therefore radius:

$$\mathbf{t_c = 1/(6D_{rot}) = V\ \eta/kt}$$

$$\mathbf{Volume = 4/3(\pi)r^3}$$

$\eta/kt = 0.01\ poise/(1.38x10^{16} * 293K) = 2.4732 \times 10^{11}$

where η is the viscosity and r is the dipole radius

This provides a relationship between r and t_c

Thus, we predicted that the characteristic DRS relaxation frequency of maximum dielectric loss would be related to the dipole rotational correlation time. This is because the AC fields applied in DRS cause the dipolar molecules to rotate, with a maximum interaction likely to occur at the natural rotational frequency of the molecules.

We first applied this equation to data in the literature. For instance, the expected relaxation frequency of myoglobin is 10 MHz, amino acids are 160 MHz, and water is 16 GHz. We plotted correlation times against particle diameters for several large molecules of varying sizes (hemoglobin, bovine serum albumin, green fluorescent protein, dendrimers) and theoretical particles. The resultant plot clearly demonstrates the correctness of the Stokes-Einstein-Debye equation for large biomolecules. We also plotted the characteristic frequency for the DRS signal for one of the molecules (pACCA) used in this study. The fit was good. This exercise provides us with some confirmation of our understanding of the DRS phenomenon and permits us a basis to predict the characteristic correlation frequency from the molecular size.

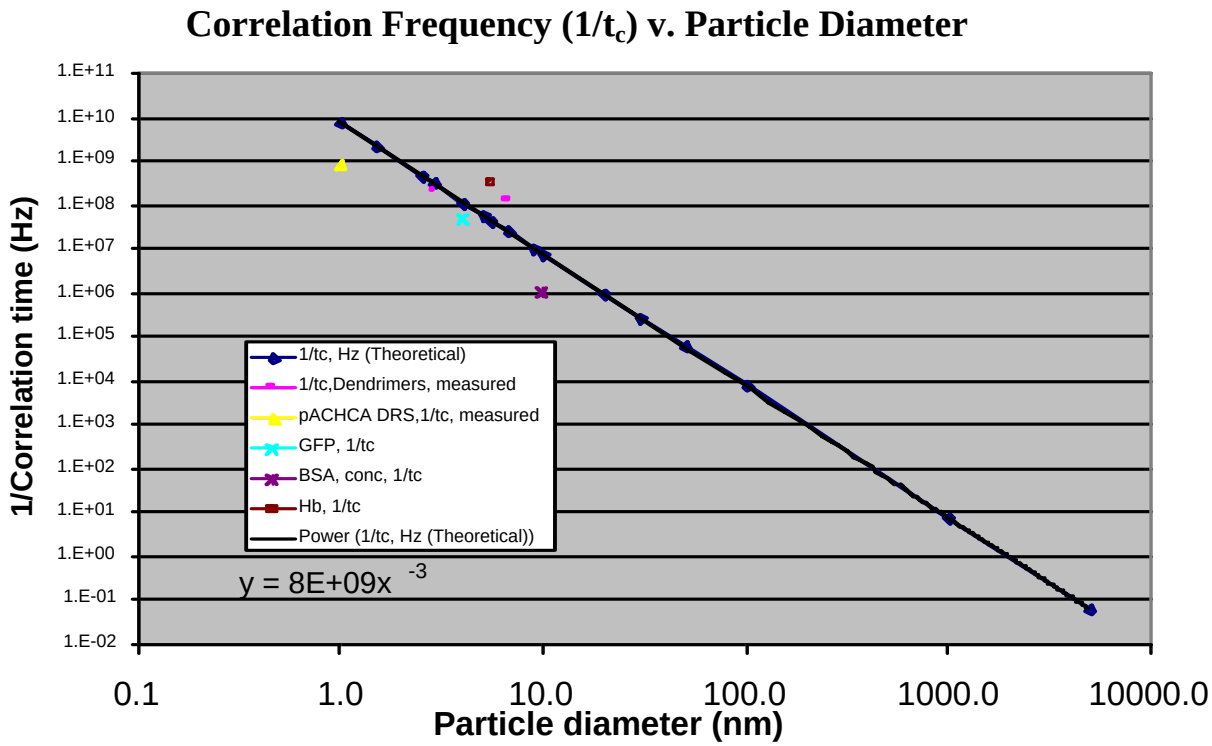

INSTRUMENTATION

The project requires specialized electronic equipment that operates at frequencies into the microwave region. DRS requires measurements of the relative permittivity (e') as a function of frequency and its derivative, dielectric loss (e''). The frequency of maximum dielectric loss is known as the "characteristic frequency" or the "relaxation frequency." A "probe" transmits a signal into the material under test and the reflected response from the material is then related to its dielectric properties. From the reflected power the relaxation frequency of our dipolar molecules can be characterized.

The Agilent (Hewlett-Packard) model 85070M "Dielectric Probe Measurement System" in the CMU Center for Advanced Fuel Technology (formerly the Microwave Center) was used for our initial investigations. The system comprises a model 8753D network analyzer, a model 85070B dielectric probe and model 85071B materials measurement software, which together form the dielectric characterization system and is useful across RF and microwave frequencies. Primarily targeting liquids and solids, this system can be used to determine the complex dielectric permittivity (dielectric constant), loss factor, loss tangent, or Cole-Cole diagrams from 200 MHz to beyond 3 GHz for many materials.

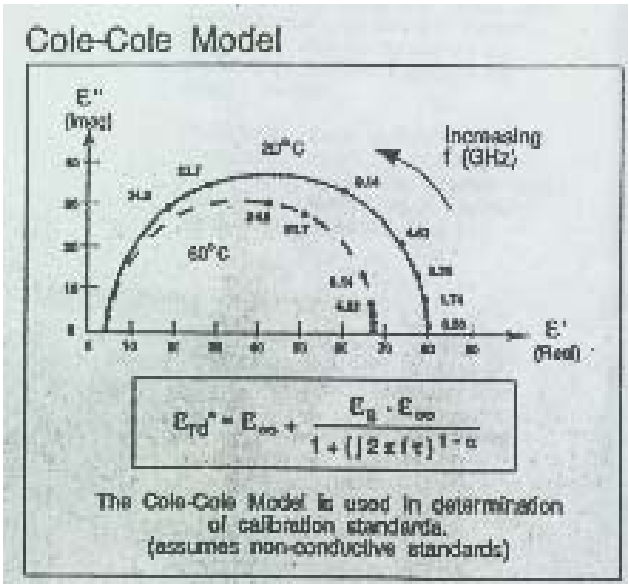

Impedance ***Z*** is measured by the instrumentation and relates as:

$$Z = R + jX$$

where **R** is resistance, ***X*** is reactance, and ***j*** represents the imaginary component and is used to represent a complex number. The real component of impedance, **R**, is dominated by the resistive components in the IDEs while the imaginary component, ***X***, is dominated by the capacitive components of the IDEs. Reactance is an expression of the extent to which an electronic component, circuit, or system stores and releases energy as the current and voltage fluctuate with each AC cycle. Reactance is expressed in ohms. It is observed for an alternating current but not for a direct current. When AC current passes through a component that contains reactance, energy might be stored and released in the form of a magnetic field, in which case the reactance is inductive (denoted ***+jX***); or energy might be stored and released in the form of an electric field, in which case the reactance is capacitive (denoted ***-jX***). Conceptually, one can think of R along the real axis, and X on the imaginary axis of a complex graph.

Capacitors are reactive, they can store and release energy, and current through a capacitor is phase shifted -90 degrees with respect to the voltage. Thus, it is not in the same phase as resistance, therefore ***j*** is used to represent the component that is out of phase.

To relate the impedance to relative permittivity (e') and the dielectric loss (e''), the impedance equation above can be written as the following:

$$1/Z = Y = G + jB$$

where **Y** is the admittance, **G** is called the conductivity, and **B** is the susceptance.

We know that:

$$G = s\,(A/l)_{eff}$$
$$B = \omega\,\varepsilon\,(A/l)_{eff}$$

Where **s** is the conductivity, **ω** is the angular frequency, **ε** is the complex permittivity. The effective area, $(A/l)_{eff}$, is the constant that accounts for the electrode geometries where A is the electrode area and l is the distance between the electrodes. We can substitute the following for the complex permittivity:

$$\varepsilon = \varepsilon' - j\varepsilon''$$

Where **ε** is the complex permittivity, **e',** is the relative permittivity, and **e''** is the dielectric loss.

We can solve the equations for e' and e'', to show that:

$$e' = s\,B / (G(0)\,\omega)$$
$$e'' = e'\,(G-G(0)) / B$$

Permittivity describes the interaction of a material with an electric field:

$$K = e^{'} = \varepsilon / \varepsilon_0$$

Where *K* is the dielectric constant, $e^{'}$ is the relative permittivity and ε_0 is the permittivity of free space (8.854 pF/m). The complex dielectric constant is made up of a storage component and loss components. The loss components are made up of conductive and dielectric loss (e'') components.

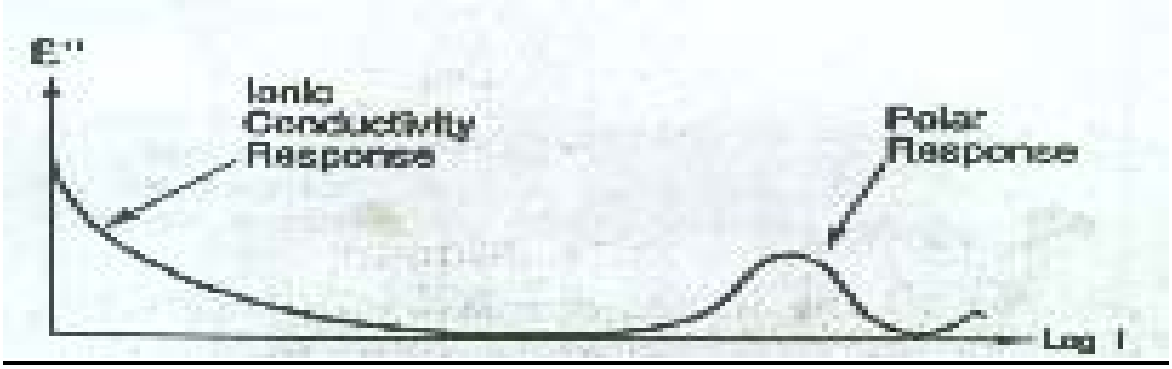

The dielectric probe is used to measure the intrinsic electrical properties of materials—dielectric properties—in the RF and microwave frequency bands. It allows measurement of the complex dielectric constant (relative permittivity) of liquids, the dielectric loss factor (loss tangent). The probe features a hermetic glass-to-metal seal, which makes it resistant to corrosive or abrasive chemicals. It withstands a wide –40°C to +200°C temperature range, which allows measurements versus frequency and temperature. This is an important variable, since the dielectric properties of materials can vary significantly as a function of temperature. Measurement accuracy for the probe is typically 5 percent.

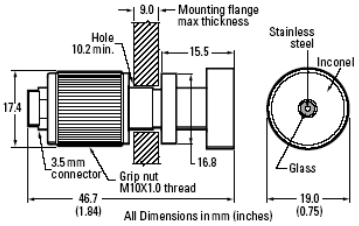

Unfortunately, this standard probe is designed for relatively large samples, not molecular biologic quantities. We designed and built a sample well appropriate for 500 ul samples or less. Leads are isolated, short, and matched. Further testing indicated that we were reproducibly able to measure small volumes down to 100 ul. We were able to achieve replication of typical DRS spectra with this instrumental setup, but complex dielectric permittivity generally exhibits a dependence or sensitivity to sample geometry and we anticipated further optimizing this probe.

We recognized that we were attempting studies with crude un-optimized instrumentation, but the system is very sensitive to specific geometries and other aspects of the instrumentation. We had hoped that if we could detect a signal we could optimize our instrumental setup for a practical analysis.

Our investigations were performed at 25 degrees centigrade and scanning the frequency range of 60 Megahertz to 6 Gigahertz. Resultant plots were corrected by subtraction of the water signal.

Traditional DRS is an insensitive technique requiring high concentrations of analytes. We had hoped that we could address this sensitivity issue by specifically engineering probe molecules to suddenly produce large signals upon hybridization of probe to target. We thought that if we could accomplish this, then we could model and optimize the system that could eventually lead to a practical DRS STR microchip.

NON-DNA BIOMOLECULAR ANALYTES

We initially tested non-DNA biomolecules to verify that we could obtain appropriate DRS spectra. We pilot tested 1,3 butanediol as a small molecule with a known DRS spectra to verify the DRS instrumentation, and found that we could reproduce a relaxation spectra as published in the literature. Then, to see whether changes in spectra from our instrumentation made sense and to gain a sense of range, we compared glycine, a 2-carbon amino carboxylic acid, to epsilon-aminocaproic acid (EACA), a 6-carbon amino carboxylic acid, at two different concentrations. EA yields a stronger loss spectrum than glycine. Although the dipolar charges of glycine and EACA are equal in magnitude, the increased charge separation of EACA (and thus greater dipole moment) results in an increased signal. Also, The relaxation frequency of 1 M EACA (646 MHz) is considerably lower than that of 1M glycine (3.74 MHz), again, consistent with the larger size of the dipole and a longer correlation time for rotation of the bigger molecule. Furthermore, one-tenth molar solutions yield 1/10 the intensity of dielectric loss of 1 M solutions at the same frequencies demonstrating the potential for quantitation by DRS analysis. One-tenth molar solutions also relaxed at slightly higher frequencies perhaps due to less inter-molecular interaction (lower viscosity).

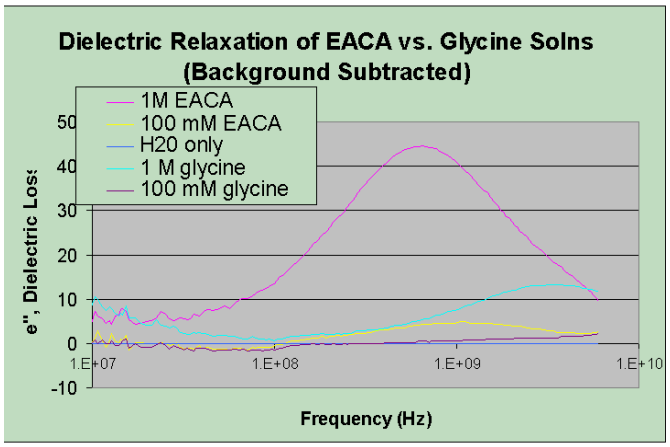

We further explored concentration effects through a serial dilution study of EACA to establish crude sensitivity limits for our assay. We varied the concentration of the small organic dipole EACA from 3.9 mM to 1 M. Plotting superimposed spectra demonstrated that the signal increased and sharpened with concentration, as expected. The corrected dielectric loss (e'') varied from near 0 to 45 units with increasing concentration. A discernable peak was first seen between 16 and 31 mM concentration. Increasing concentration caused the peak to shift slightly to lower frequencies (from approximately 1 GHz to approximately 800 MHz), presumably due to increased viscosity of the solution.

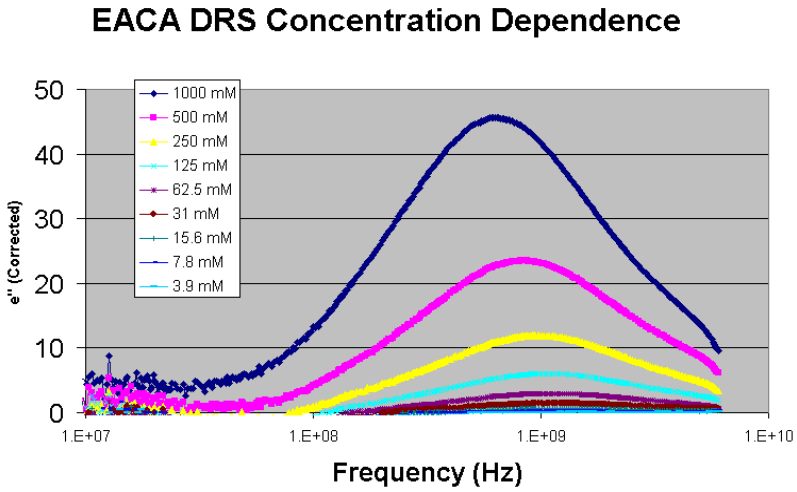

We plotted the dielectric loss (corrected for water) at 630 MHz against concentration using two different molecules (EACA and pACCA–explained below). The strength of signal decreased linearly with concentration. We obtained a linear relationship (Y = 0.046X – 0.3) down to the lowest concentration of 4 mM with a correlation coefficient at 0.9988. This suggests potential sensitivity in the physiologic range.

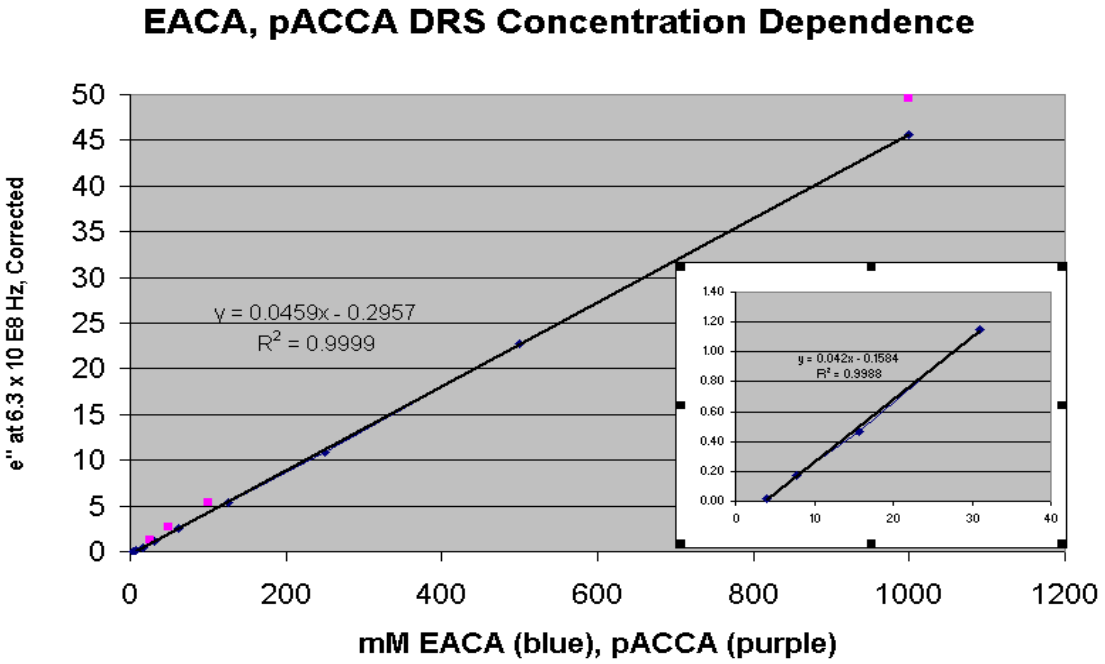

We then further explored dipole length changes. We performed DRS on amino carboxylic acids of varying chain lengths to quantitate the effect of increasing chain length on the resonant frequency and intensity. Gamma amino butyric acid (4 carbons), 8-amino caproic acid (8 carbons) and 12-amino dodecanoic acid (12 carbons) were first studied and then further expanded our investigation by sequentially increasing carbon length from 1 to 10 carbons at 1M and 100mM concentrations. We compared the characteristic frequency (the frequency of maximal signal) and the dielectric loss (e'') with

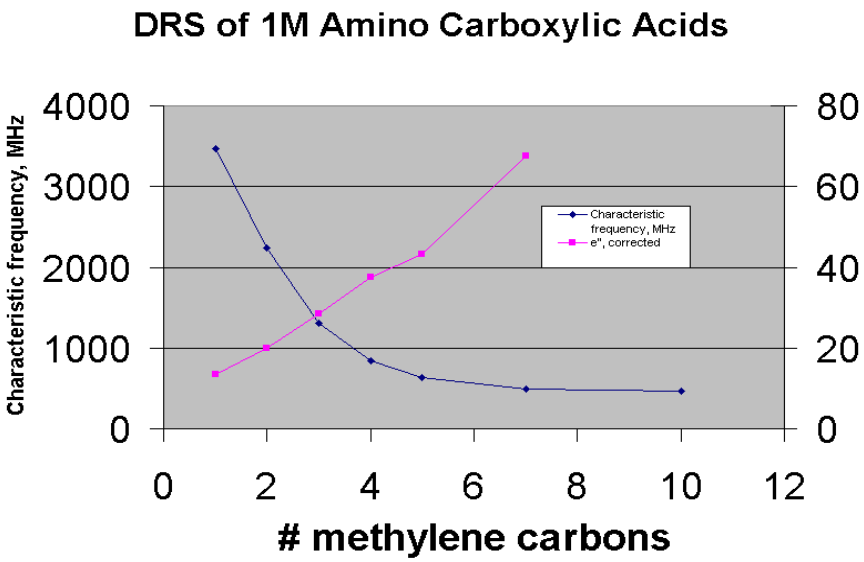

the increasing dipole length. The results confirm and more clearly show that signal strength increases with dipole length and the frequency of relaxation decreases.

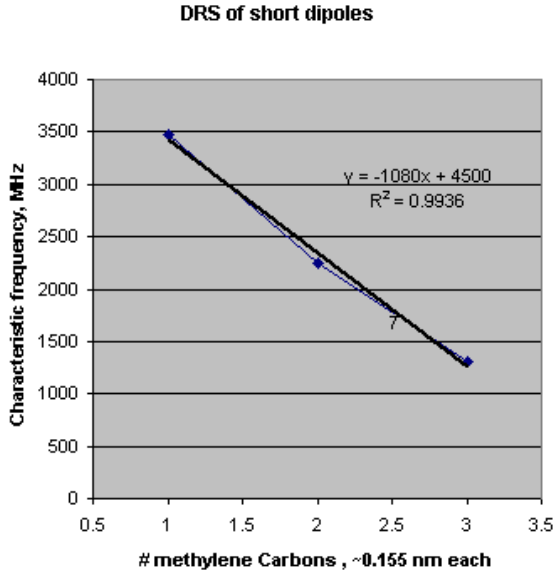

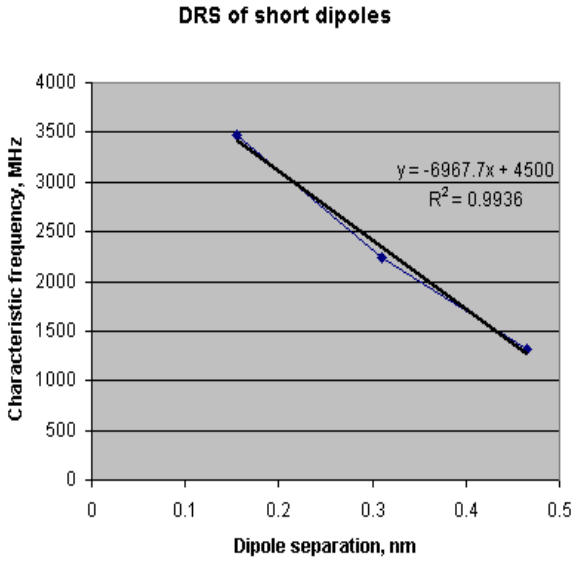

The relaxation frequency varies from 3.5 GHz for single carbon dipoles to 500 MHz at seven carbon unit dipoles. This frequency declines with increasing dipole length in an exponential fashion, as would be expected for slower rotation of longer dipoles. This relationship seems to break down for molecules with greater than about 5 to 7 methylene carbons, probably due to flexibility of the long carbon chains. Simultaneously, the magnitude of the dielectric loss (e''), varies linearly from about 10 to 70 units. This is expected since dipole strength is linearly related to charge separation: $\mu = qR$.

We also investigated the effect of dipole flexibility on the DRS spectra by comparing epsilon amino caproic acid (EACA) to para-aminocyclohexane carboxylic acid (pACCA). Both molecules have a six-carbon unit length, but the pACCA is rigidized and the EACA is not. The rigidized dipole, pACCA, produced a 10% greater peak height (50

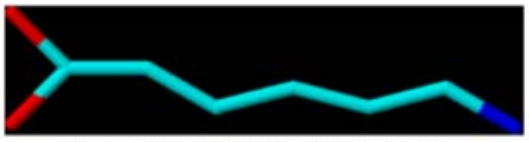

Epsilon Amino Caproic Acid (EACA)

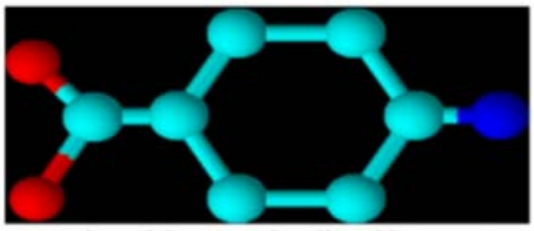

p-Aminocyclohexane Carboxylic Acid (pACCA)

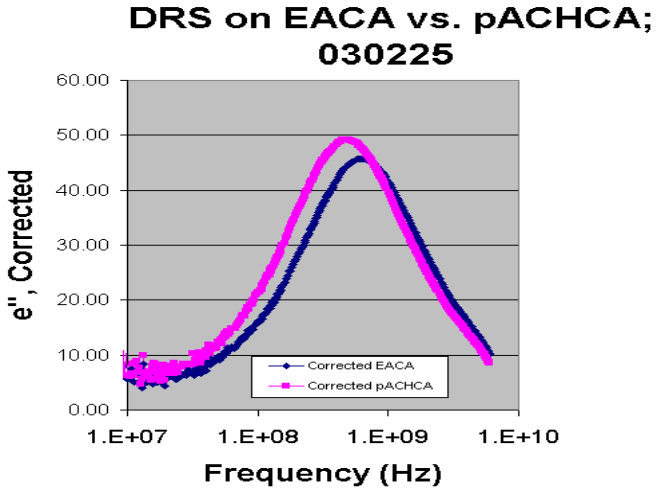

units) at 1 M concentrations than the non-rigidized dipole, EACA, (45 units), but apparently at the same relaxation frequency.

These results confirm that our procedure and equipment are effective in detecting dipoles from a variety of compounds. Consistent with DRS theory, we were able to increase signal by increasing the separation of the charges. Furthermore, they provide us a molecular "yardstick" against which we can test our new probes.

We measured the interference caused by salt (ionic relaxation) on dipolar DRS signals. The graph below superimposes the salt signals of normal PBS solution and serial dilutions on top of a 1 M EACA signal as well as a water signal that is subtracted from the other curves. Water is separately plotted. This clearly illustrates the masking of the analyte signal by the salt ionic signals at physiological salt concentrations. The signal window is bounded by salt on the left and water on the right, but it appeared a millimolar analyte signal could be detected within this window—assuming the peak frequency did not shift too far to the left and the salt concentration was sufficiently low.

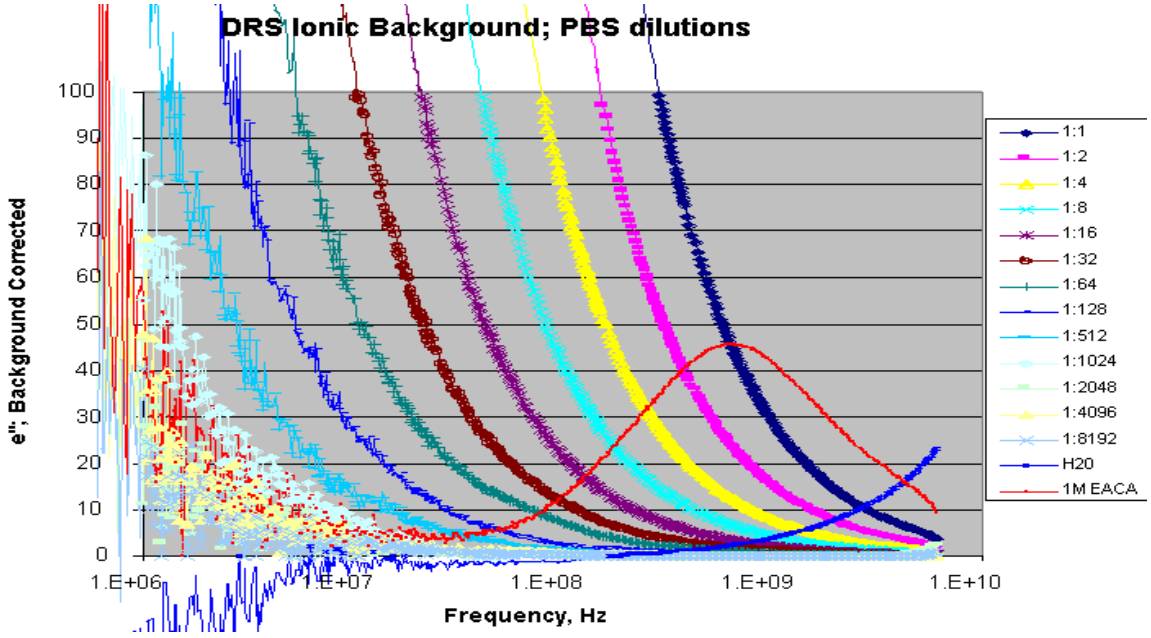

PNA PROBES

We proposed to use a DNA probe with a charge on one end for a DNA target strand with an opposite charge on the opposite end, to create a very large dipole moment when the two strands hybridize. An N-terminal polylysine can provide a large positive charge while a C-terminal polyglutamate could provide a large negative charge. Since no opposing charge is on either single-stranded fragment and both are relatively flexible, there is no significant dipole moment until the moment of duplex formation. In other words, a large signal should be produced with each hybridization event with little background signal from the unhybridized label. For repetitive sequences, like STRs, it

may be an advantage to engineer a two-probe system that bind to the shoulder regions and thus prevent nonspecific hybridization within the target (out-of-register hybridization). Alternatively, two DNA probes may be designed to hybridize with adjacent sequences on the DNA target. Yet another possibility is to use a probe with opposing charges at each end and forming a hairpin that will open up upon binding to its target creating a sudden dipole moment as the charges move away from each other. This is analogous to the molecular beacon technology that employs a fluorophore and quencher rather than charge tags. The advantage of this system, as of the molecular beacon system, is that the target does not need to be labeled.

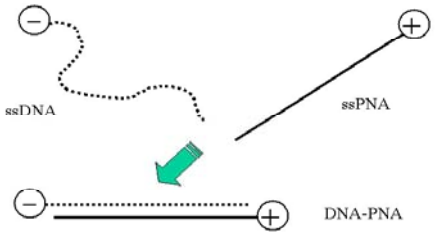

Originally, we used Peptide Nucleic Acid (PNA), a synthetic analogue of DNA, rather than conventional DNA probes because PNA has a more rigid structure and lacks the negative charges from the sugar phosphate backbone. However, instead of using linear probes, we decided to produce a PNA hairpin probe. The two positive and two negative charges in close proximity will spread to 50 Å upon hybridization to its target. The PNA sequence was synthesized by standard solid-phase methods and purified by reversed phase HPLC. MALDI-TOF mass spectrometry was used to verify the identity of the PNA (calculated mass = 4202.0). UV melting analysis indicated that the PNA did fold into a hairpin structure with a melting temperature of 76.8 ºC. Addition of the complementary DNA yielded a PNA-DNA duplex having a melting temperature of 68.2 ºC.

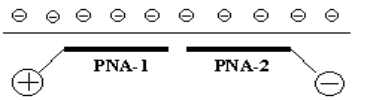

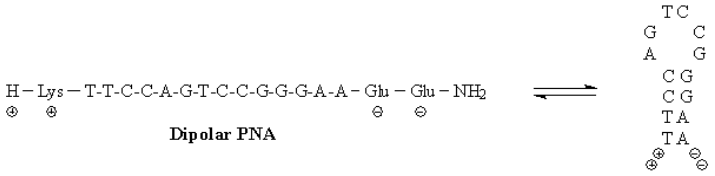

We compared the DRS readings of 1 uM PNA-DNA hybrids to PNA, DNA, buffer solution, and double distilled water. The results were disappointing; no signal was detected. All samples were identical or very close to ddH2O. The dielectric loss was about 78 and quite stable until in the low gigahertz range (beginning ~1 GHz) where water relaxes. We saw no dielectric effects from the DNA, the PNA or the PNA-DNA.

We considered that the concentration of the PNA-DNA was too low and the relaxation signal possibly swamped by the relaxation signal of the water. Thus, the concentration of the PNA was increased to 100uM. However, the PNA-DNA mixture, which was the PNA-DNA hybrid, precipitated out of solution. We attempted to avoid precipitation by combining the DNA and PNA at different temperatures; we attempted to melt and re-anneal the PNA-DNA mixture at temperatures up to 100^{o}C, to no avail.

We then redesigned the probes to minimize precipitation by minimizing the PNA size, addition of multiple ionic charges placed on the end of the probes, and creating a DNA overhang upon hybridization. Specifically, we used a peptide-PNA conjugate (NH_2COLys-Lys-CTCGTGTC-NH_2 with only two positive charges) to bind to a series of different sized complementary DNA oligonucleotide targets [5'-GAGCACAGATTA-3' (4 base overhang), 5'-GAGCACAG-3' (match), 5'-CACAGATTA-3' (3 base underhang)]. At 250 mM PNA, an 8 base pair complement precipitated and so did a 5 base underhang, but a four base pair overhang was soluble. We replaced the hydrophobic and poorly soluble PNA entirely with DNA, which because of its negatively-charged phosphate background is far more hydrophilic. We created DNA-peptide conjugates in which a polylysine tail provided the positive charge tag. We also reduced the number of end charges to reduce the dipole-dipole interactions that may result in complexing and precipitation. A twelve-charge tail requires 140 mM salt concentration to maintain solubility, whereas a six-charge tail requires 100 mM salt concentration to maintain solubility. These strategies did not result in significantly improved signal.

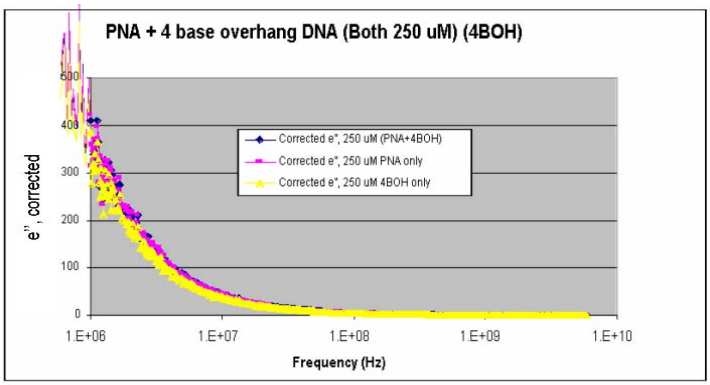

DNA PROBES

We abandoned the PNA probe chemistry in favor of DNA chemistry to maintain solubilization and avoid precipitation. We were unable to use PNA probes at sufficiently high concentration without its precipitating out of solution. At lower concentrations, we did not observe a signal which we thought was buried within the salt signal (the PNA required high salt to maintain solubility as did our 6 positively and 12 positively charged peptide-B conjugate combined with A). DNA, because of the negative charges along the sugar phosphate backbone, is inherently more hydrophilic than PNA, which lacks these backbone charges.

We decided to try linear DNA probes with charge tags. Two complementary DNA probes of 15 and 25 base pairs were synthesized; either unlabeled (to serve as controls) or 5' amino labeled (a positive charge) with the complementary sequence 5' labeled with Cy3.5 dye (which has 3 negative charges). Combinations of labeled and unlabeled sequences were tested. In no case was any signal observed due to hybridization and formation of a dipole. All DNA sequences were tested at 100 uM, which is much less than the amount required for a signal using small organic dipoles, due to the cost of the DNA probes.

We constructed hybrid molecules using small peptides, and DNA. This was accomplished using a heterobifunctional crosslinker. The advantages of this approach include: 1) it is possible to construct engineered molecules by adding one amino acid and one DNA base at a time, 2) custom DNA oligomers and peptides are commercially available at a relatively low cost and, 3) coupling chemistry is straightforward. An example of such is**:** NH2 – $(LYS)_5$ – PRO – $(LYS)_5$ – TAC-GAG-TCC-TGG-AAC. We attempted to minimize concentration of positive charges used to minimize non-specific binding. We recognized that the hybrid probe molecules are themselves dipoles and thus will give dielectric loss signals. Our results with these DNA probes were equivocal.

To increase the possible signal strength, we increased the charges. Two amino-terminal 15-mer peptides: a short peptide [R-KKPKKPKKCysteine-SH] with 6 net positive charges and a long peptide [R-KKKPPKKKPPKKKPPKKKCysteine-SH] with 12 net positive charges were conjugated to DNA (15 negative charges) using a heterobifunctional crosslinker. Both conjugates were made in high concentration for the experiments (~100 mM). Phosphate buffer/NaCl was required to keep them soluble. Unfortunately, the salt obscured any DRS signals.

We decided to lower the number of charges and thus the dipole-dipole interaction in hopes of increasing concentration while maintaining solubilization. Moreover, we also hoped to improve our chances of demonstrating a signal through the creation of a dynamic shift in the signal by hybridization in accordance to our original conception. Thus, we performed a DNA hybridization study ("mixing" experiment) at the higher concentration. An "A+1" 16mer oligonucleotide will complement to a "B-NH_3^+" thus forming a negatively charged overhang on one end and a positively charged amino group at the other end to form a dipole (A+1 and B-peptide conjugate). Unfortunately, this strategy too was unsuccessful in creating a detectable DRS signal.

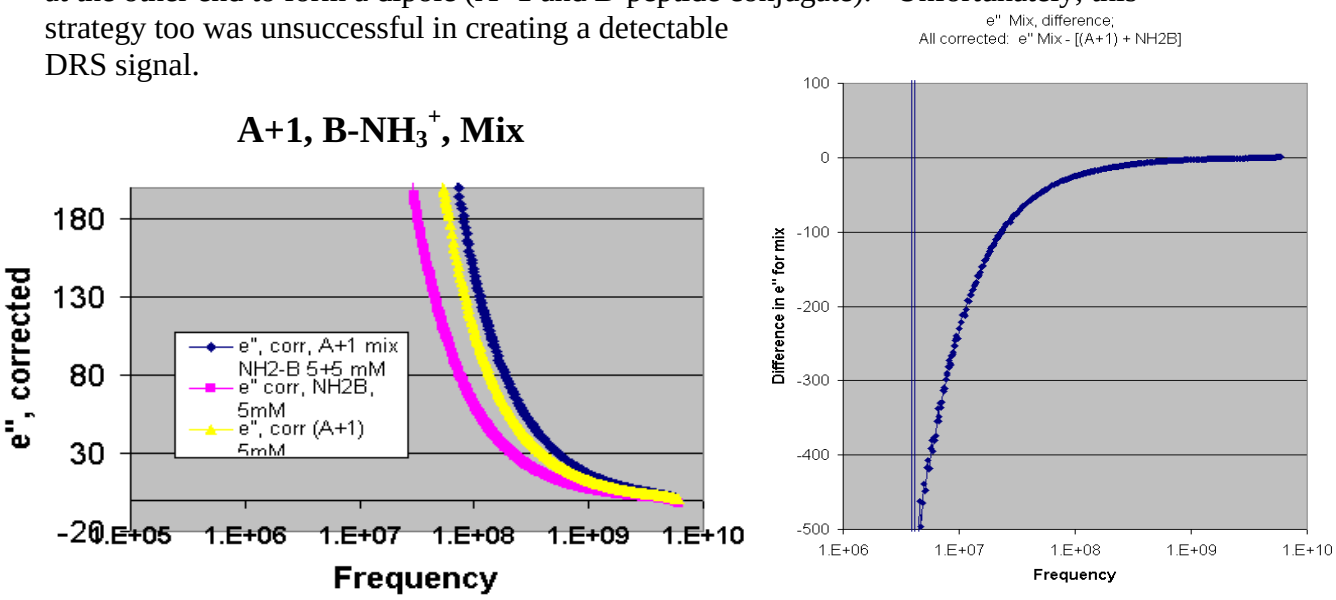

Thus, after conducting our nucleic acid studies we were left with the impression that there is a window bounded by the water relaxation frequency at the high end and by ionic salt signals at the low end. The concentrations of dipoles necessary to see these signals are quite high, generally in the millimolar to molar range. The maximal concentration of DNA that we had been able to keep in solution and test was 250 uM, however our results using small organic dipoles suggest a need for a concentration of approximately 4 mM to detect with our original instrumentation. Unfortunately, high concentrations of analyte required high concentrations of salt that masks their relaxation signal. This may well explain the paucity of work on organics in the literature. Our data from our small nonDNA biomolecules suggested that we were approximately one order of magnitude below the salt signal.

COUNTER ION SUBSTITUTION

DNA molecules are hydrated in buffer solutions with salt ions, e.g., NH_4^+, Na^+, and K^+. The cations are attracted to negative charges on the DNA molecule, particularly cations to the negative phosphate groups on the backbone; this sheath is surrounded by a region of anions to form a double layer. Water molecules also orient and align themselves around the DNA molecules. Collectively these are known as the counter-ion sheath. The small ions from Brownian motion and other forces will temporarily move in and of the sheath, temporarily exposing the DNA molecule itself. The authors of the NIST study (mentioned above) believed that the signals of DNA solutions seen by DRS are really due to this counter-ion sheath.

The predominant counterions for our pure DNA oligonucleotides are ammonium ions which are required for solubilization. However, they appeared to mask the signal of interest. These buffer salts were kept at minimal concentrations by manufacturer desalting and even in-house gel filtration chromatography with distilled water. Nonetheless, the salt signal still appeared to be overwhelming and no DNA signal was seen.

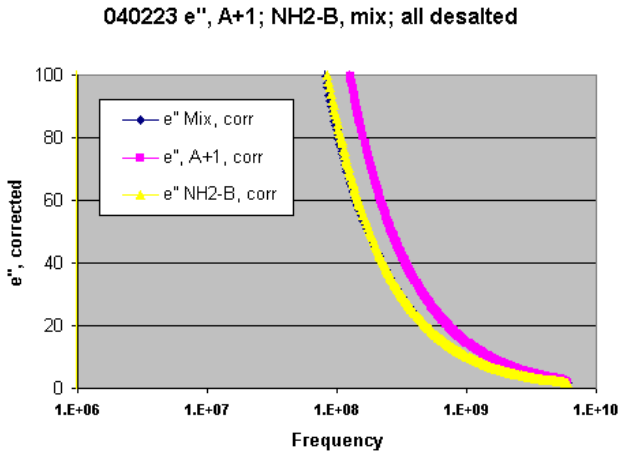

A strategy for decreasing the salt signal is to replace the salt ions with larger polyvalent non-salt counter ions, such as urea, spermine or protamine. These ions will have a significantly lower relaxation frequency and thus open the window where we hope to detect analyte biomolecules of interest. The NIST group added spermine to their samples to decrease the counter-ion sheath signal. We decided to investigate the use of protamine, spermine, and two diamines to displace the salt ions in hopes of making the DNA signal visible. We conducted DRS analysis on the DNA samples with and without each of the amines using the traditional instrumentation setup to look for the appearance

of a DNA signal (or stronger DNA signal) or a weaker salt signal. Unfortunately, after mixing a 2-fold excess of spermine with the DNA and washing via a 3000 MWCO spin column, the A+1 oligo was insoluble, and would not go back into solution, even with heating. Thus, we were unable to obtain DRS spectra of these samples.

SALT SIGNAL

Because the signal from the salt ions in the solution is so massive and easily detected, we decided to look at this signal as a method to detect DNA hybridization. In other words, we considered that it may be more fruitful to look for the release of salt ions of the counter ion sheath from hybridization events than directly from signals of the DNA molecules themselves. We compared the DRS spectra of DNA before and after hybridization by its complement, as well as after denaturation by the addition of formamide. We reviewed the data from the mixing experiment above (DNA A+1 solution & DNA NH_2-B) for a change in the salt signal. Unfortunately, not only was no DNA signal seen but also no change in the salt signal was recognized.

MICROGAP IDEs

Yet another strategy is to increase our detection sensitivity. We attempted to improve the signal through our instrumentation by concentrating the field effect. We knew that the signal in bulk solution would exponentially dissipate with distance from the electrodes. The current probe station in our experimental setup was designed for bulk solutions of non-biomolecular types. While it may work well for bulk mixtures, it is in all likelihood suboptimal for this current intended use. We intend to increase the field strength by use of micromachined interdigitated electrodes (IDEs). The gaps between such electrodes are microscopic rather than the macroscopic of our conventional probe station. While they are routinely used for a variety of applications, manufacture is not trivial. There are issues of electrical connection, how to cover the IDE with sample, matching impedance to the instrumentation, and parasitic losses.

The IDEs cannot be tested using the traditional microwave instrumentation that we had used to perform other experiments. That original equipment uses a specially-designed (50 ohm) probe to measure the permittivity of liquids, but is not setup to connect to our newly manufactured IDEs. We used another network analyzer (CMU MEMS laboratory) and then matched the instrument to the greater impedance of the IDEs. Resistive and capacitive components between the network analyzer and the interdigitated electrodes had to be zeroed out to measure a pure capacitance value that relates to the imaginary component of the permittivity.

This instrument however was not set up for DRS testing and did not automatically output permittivity results, instead it measured impedance of reflected transmitted waves from which the relaxation frequency of our dipolar molecules must be derived.

We spent considerable effort in understanding how the impedance measurements of the network analyzer relate to permittivity (e') and dielectric loss (e''). The Network

Analyzer output from our IDEs is read in terms of S11 reflectance coefficients. We needed to convert the S11 coefficients to impedance (Z). This was done in the following manner:

S11 = Z-Zo / Z+Zo

where *Z* is the input impedance, and *Zo* is the characteristic impedance of the Network Analyzer, 50 ohms.

Rearranging:

Z = Zo (1+S11) / (1-S11)

Substituting the real and imaginary components in for $S_{11:}$

$$Z_{IN} = Z_O\left(\frac{1+R+jX}{1-R-jX}\right)$$

After multiplying by the complex conjugate to separate real and imaginary components:

$$Z_{IN}(REAL) = Z_O\left(\frac{1-R^2-X^2}{(1-R)^2+X^2}\right)$$

and

$$Z_{IN}(IMAGINARY) = Z_O\left(\frac{j2X}{(1-R)^2+X^2}\right)$$

The real component of impedance, Z_{IN}(real), is dominated by the resistive components in the IDEs while the imaginary component, Z_{IN}(imaginary), is dominated by the capacitive components of the IDEs. The IDEs can be modeled using a series and parallel configuration of resistors and capacitors as shown below:

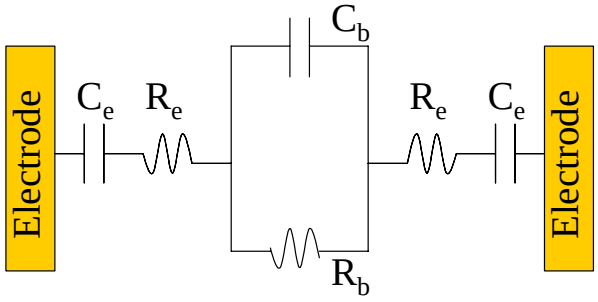

C_b and R_b represent the capacitive and resistive components of the bulk solution, respectively. While C_e and R_b represent the capacitive and resistive components of the ionic double layer at the electrode surface, respectively. Since we only want to measure

the capacitive and resistive components of the IDE only and not any parasitics, we have calibrated to remove all circuit elements up to the interdigitated electrode fingers. The

$$C = \frac{N A e'}{l}$$

dielectric relaxation phenomena can be identified by the change in permittivity, which is embedded in the capacitive component as shown in this equation:

Where N = the number of fingers in the interdigitated electrode, A = the area of the electrodes, e' = the permittivity, and l = the thickness of the dielectric.

We are able to relate the measured capacitance to the reactive component of the impedance by using this equation:

$$X = \frac{1}{2 \pi f C}$$

Using these sets of equations, we can correlate the measured impedance values back to changes in the permittivity and thus observe any dielectric relaxation.

We successfully fabricated an acceptable micro-IDE. This electrode array is composed of gold film (5000 A) on a titanium base (100 A), deposited on an oxide-coated silicon substrate. We can reliably generate a gap size down to 2 microns, but created devices with 5-micron gaps that should generate field strength of 8.2×10^5 V/m. We have also perfected the external wire connects. We connected the array to an appropriate network analyzer to measure impedance over a wide range of frequencies sweeping into the Gigahertz range. To remove parasitics from the bondpads and leads, a calibration was performed using a short, open, and load set that is also on the silicon substrate. We believed that it is possible to gain perhaps three orders of magnitude in signal sensitivity and thus, we hoped to begin to see the signals that we were thus far unable to detect.

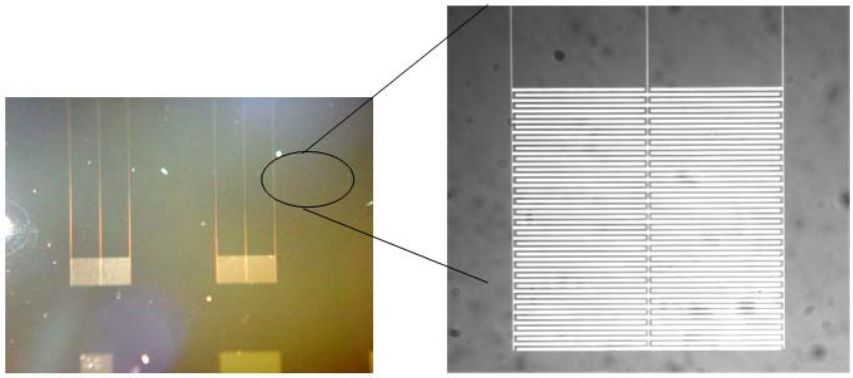

MicroIDEs require that the substrate be entirely insulating, such as glass, in order to avoid leakage of the electric field to the substrate. Unfortunately, we found that the interdigitated electrodes (IDE) had a parasitic capacitance between the metal electrodes to the silicon substrate, which is situated underneath the insulating layer of silicon

dioxide. We calculated the capacitance from the electrodes to silicon to be 40,000 pF, while the capacitance between the electrodes in air is only about 100 pF. Therefore the parasitic is close to 400 times greater, thus the majority of the electric field is directed downward instead of between the electrodes, as shown in this figure:

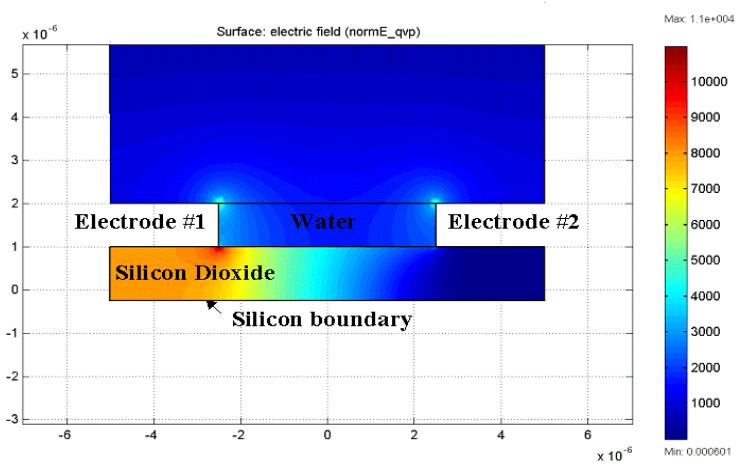

Microgap IDE modeling

NANOGAP IDEs

While working on our micro-IDE chip, we found through our modeling efforts that we can significantly increase our field strength as well as achieve other advantages with still further reduction in electrode gap size to the nanoscale. Theory dictates that 80% of the field strength between interdigitated electrodes is confined to a height above the electrodes that is equal to the gap between the electrodes. Thus, by building very tiny, closely spaced, electrodes it is possible to largely confine the interrogating field very tightly. The model predicted that a gap of 100 nanometers should produce a field strength of 1.8 x 10^8 V/m.

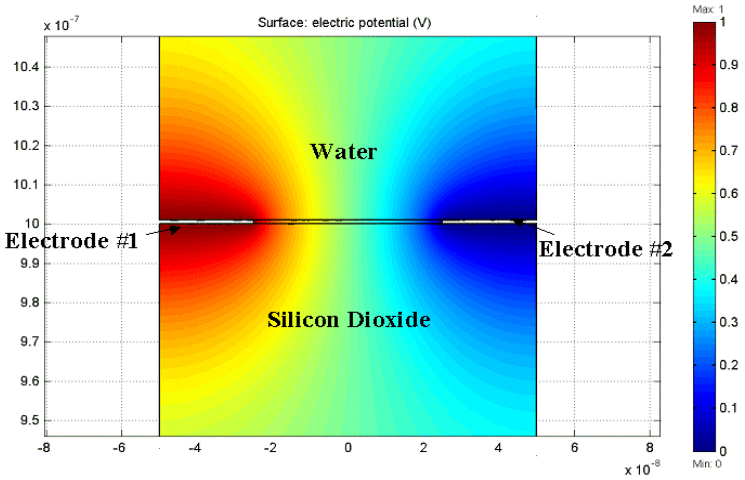

Nanogap IDE modeling

Thus, we anticipated a sensitivity increase of up to three orders of magnitude over micro-IDEs. However, the number of molecules sensed will also be correspondingly fewer. The electric field created by an array of nanoelectrodes will extend out more into the bulk fluid in a relative sense, therefore actuating more molecules. Thus, the sensitivity may or may not scale advantageously. Furthermore, the larger electric field intensity allows smaller dipole molecules to be rotated when an AC signal is applied. Moreover, nano-IDEs do not require an insulating substrate, because the parasitic capacitance becomes trivial. The calculated capacitance between electrodes that are 50 nanometers apart is approximately 300 pF while the parasitic capacitance is only 2.8 pF. Thus, we believed that such nano-IDEs might likely prove advantageous, but that experimentation would have to verify this.

Using E-beam lithography, we designed nano-electrodes with gaps of 20 - 35 nm. Such a device is at the limits of current nanofabrication. We do not have the facilities to produce such a device at CMU. We spent considerable effort in attempts to manufacture the device using the Penn State University nano laboratory and their E-beam lithography instrumentation; however, after literally months of frustration, we abandoned this path in favor of the Cornell nanofacility, arguably the most advanced in the world. We, in fact, successfully achieved the manufacture of a nano-IDE with 80nm electrode widths and 160nm gaps without electrical shorts.

Individual nanometer scale interdigitated electrodes (nano-IDE's) were diced from a wafer containing a batch of nano-IDE's. Gold bond pads and connecting rails were added at CMU using a Kurt Lesker sputtering system. All nano-IDE chips were cleaned in an acetone bath, under sonication in a sonicating water bath. We initially used 5 minutes but this was decreased to 2 minutes when one of the nano-IDE's was damaged by the longer sonication. The chips were rinsed with isopropyl alcohol, then with deionized water. Finally they were gently dried with compressed air. Short, open, and load devices were also fabricated for calibration of the network analyzer. These included shorted and open bond pads with side rails but without any nano-IDE's. All chips were examined carefully under a microscope for defects and each was tested for shorts before being used.

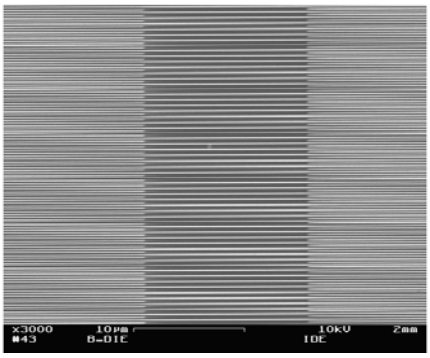

IDE with 80nm electrode widths and 160nm gaps

Measurements were performed on a Cascade Microtech Summit 6" semiautomatic pico-guarded thermally-controlled radio frequency probe station, in combination with an Agilent E8364A PNA 50 GHz microwave network analyzer, in a sealed, completely copper-clad room, at CMU. Calibration of the probes was done with an impedance substrate standard from Cascade, part number 101-190, and planarization was achieved by using a Contact Substate, also from Cascade, part number 005-018. Standard open,

short and 50 ohm load calibration was done. Furthermore, the "Nucleus" software, supplied by Cascade, was used to do open, and short calibrations on the gold bond pad and rail devices lacking the nano-IDE's was used to remove parasitics caused by these components. Each run of the device was repeated 3 times.

On initial experimentation, we were not able to wet the nano-IDE's successfully and obtained identical data for both air and water measurements. The small gaps trap air and it is difficult to get our analyte-laden buffer to wet the IDEs. This problem was solved by wetting the nano-IDE's with 95% ethanol and then gently exchanging water onto the surface of the nano-IDE's using a micropipette. The secondary problem that arises from the use of the alcohol is that the solution no longer exists as a bead, but rather floods the entire chip surface. The chips are so small and brittle that it is not easy to merely create a retention dam to hold the fluid. We were able to address this problem by carefully removing solution from the device edges using a pipette.

The resultant nano-IDE DRS spectral data for real and imaginary components is plotted below as reflected power (S11) in decibels versus frequency in Hertz for air on the left and for water, after wetting with 95% ethanol, on the right.

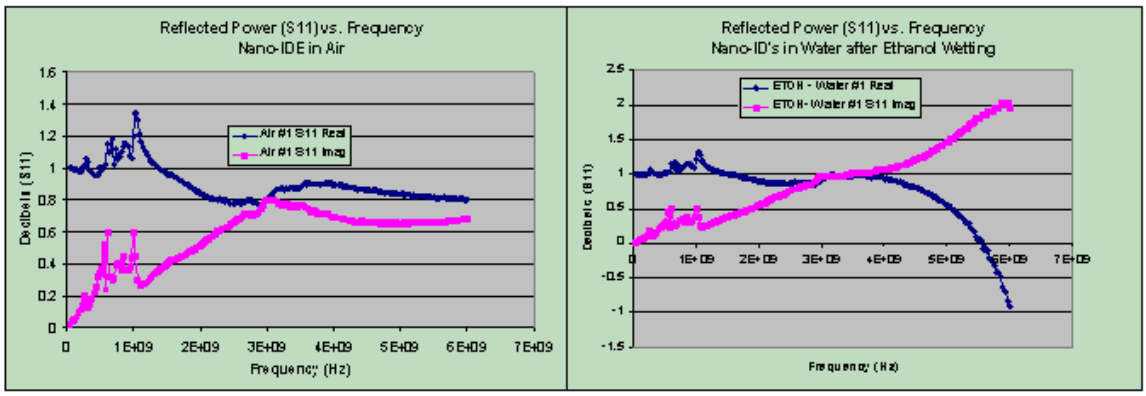

These results were obtained repeatedly by either drying the chip or by adding 95% ethanol, for 3 rounds, with virtually identical results. We were encouraged to demonstrate the ability to distinguish between air and water.

Once the system was stabilized and giving repeatable results, testing with small dipolar molecules was begun. We began with a molecule, pACCA, which had yielded excellent results in our large electrode system. We used a concentration of 330 millimolar pACCA that had given a strong signal in our original set up. Unfortunately, however, despite

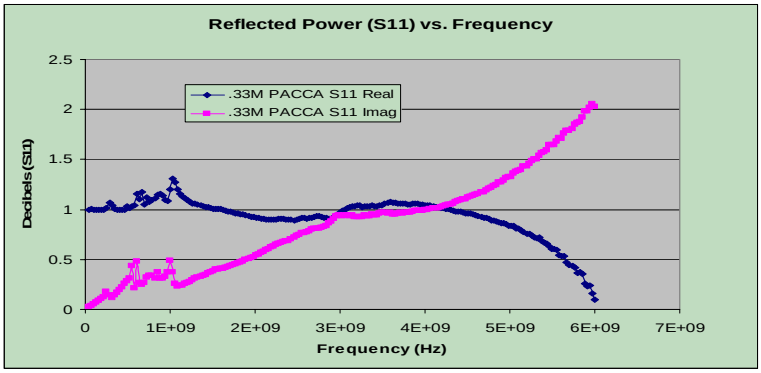

numerous attempts, we were not able to distinguish the signal of pACCA from that of water, in the nano-IDE system.

The reasons for our lack of success are unclear. The pACCA is a small molecule and should have diffused very rapidly into the nano-gaps between the IDE's and we expected that the concentration of pACCA was sufficient to ensure a good signal, based on our prior work. However, the total number of pACCA molecules in the nano-IDE gaps may have been insufficient to alter the dielectric constant of the solvent (water). It is also possible that the pACCA molecules may have non-specifically absorbed onto the surface of the gold electrodes, leaving too little in solution to be detectable.

POTENTIAL FUTURE DIRECTIONS

At this point, we decided to conclude our investigations without obtaining proof-of-concept, but having exhausted our grant funding. Nonetheless, we note there is still room for further attempts to obtain a DNA signal.

1. Electrode Charge Bias

The DRS signal falls with at least the cube of the distance of the dipole from the electrode. To date, we have been attempting to electrically interrogate the DNA molecules in bulk solution. A method of achieving local analyte concentration is through bias of the sensing electrode to increase local concentrations of analyte. It is well known that DNA can be attracted to positively charged electrodes. By positively biasing the electrode, the negatively charged DNA molecules should aggregate around the electrode, thereby increasing the local concentration of the target near the electrode and increasing the signal. By combining field confinement with electrode biasing we would expect an extremely focused system. With molecular probes close to the biased electrode and 80% of the field strength within 20 to 35 nanometers, there should be much less noise in the system due to extraneous (non-target) molecules. Of course, there is the possibility that the local concentration will result in local precipitation or concatenation of the molecules.

2. Surface-Binding

Given that signal strength drops off steeply with distance, perhaps the most likely avenue for success will come from surface binding experiments, in which a capture DNA oligonucleotide is bound to the electrode surface. A next step would be to tether the DNA through a thiol linkage to the gold surface of the IDE and then add the complementary oligonucleotide with a positive end charge (NH_2^+-B) and look for a change in the signal. A hairpin DNA probe tethered to the surface would obviate the need for labeling the target DNA.

3. Lower Frequency

We focused on the gamma and delta relaxation signals in the gigahertz frequency range, but it may be that the whole molecule rotation is better seen in the alpha relaxation signal in the tens of hertz range.

4. Dielectric Resonance Perturbation

A cavity perturbation technique can measure dielectric resonance perturbation of small samples. This involves enhanced microwave harmonic resonances to assess the complex dielectric properties based upon resonant cavity frequency shift theory, in which the real and imaginary parts of the complex electric susceptibility, $\mathbf{c} = \mathbf{e}_r - 1$, are related, through functions dependent on sample shape, to the change in cavity resonant frequency and Q.

ACKNOWLEDGEMENTS

We wish to acknowledge that the Penn State Nanofabrication Facility and the Cornell Nanotechnology Center graciously allowed us use of their facilities in our manufacture of the Nanogap IDEs.

We wish to express special thanks to Dave Purta, PhD, of the CMU Center for Advanced Fuel Technology (formerly the Microwave Center), for use of his instrumentation and for his patient teaching and advise on microwave design and conceptual understandings. Also, Tamal Mukherjee, PhD and Gary Fedder, PhD of the CMU MEMS Lab helped us to understand the electrical aspects of this work. Finally, George Lopez, PhD candidate, used his valuable time to assist in the manufacture of our IDEs and showed us how to use the electronic instrumentation. Each of these individuals also helped to edit this report, but in the end we accept full responsibility for the errors contained within. This work could not have been accomplished without such expert and always helpful colleagues.

REFERENCES

Baker-Jarvis J, CA Jones, B Riddle, Electrical Properties and Dielectric Relaxation of DNA Solution, NIST Technical Note 1509, November 1998, Radio-Frequency Technology Division, Electronics and Electrical Engineering Laboratory, National Institute of Standards and Technology, 325 Broadway, Boulder, CO 80303-3328.

Kushon SA, JP Jordan, JL Seifert, H Nielson, PE Nielson, BA Armitage, Effect of secondary structure on the thermodynamics and kinetics of PNA hybridization to DNA hairpins, J Am Chem Soc 123(44):10805-10813, 2001.

Van Gerwen P, W Laureyn, W Laureys, G Huyberechts, M Op De Beeck, K Baert, J Suls, W Sansen, P Jacobs, L Hermans, R Mertens, Nanoscaled Interdigitated electrode arrays for biochemical sensors, Sensors and Actuators B 49:73-80, 1998.

Berggren C, B Bjarnason, G Johansson, [Review] Capacitive Biosensors, Electroanalysis 13(3): 173-180, 2001.

Hefti J, A Pan, A Kumar, Sensitive detection method of dielectric dispersions in aqueous-based surface-bound macromolecular structures using microwave spectroscopy, App Phys Letters 75(12):1802-1804, 1999.

Facer GR, DA Notterman, LL Sohn, Dielectric spectroscopy for bioanalysis: From 40 Hz to 26.5 GHz in a microfabricated wave guide, App Phys Letter 78(7):996-998, 2001.

Nagel M, PH Bolivar, M Brucherseifer, H Kurz, A Bosserhoff, R Buttner, Integrated planar teraherz resonators for femtomolar sensitivity label-free detection of DNA hybridization, App Optics 41(10):2074-2078, 2002.

Schmitt R, D McCann, B Marquis, DE Kotecki, Dielectric relaxation of WO_3 thick films form 10 Hz to 1.8 GHz, J App Physics 91(10): 6775-6777, 2002.

Plum GE, VA Bloomfield, Contribution of asymmetric ligand binding to the apparent permanent dipole moment of DNA, Biopolymers 29:1137-1146, 1990.

Bonincontro A, R Caneva, F Pedone, Dielectric relaxation at radio frequencies of DNA-protamine systems, J Non-crystalline Solids 131-133:1186-1189, 1991.

Bonincontro A, R Caneva, F Pedone, TF Romano, Complex dielectric constant of arginine-DNA and protamine-DNA aqueous systems at 10 GHz, Phys Med Biol 34:609-616, 1989.

Lavalette D, C Tetreau, M Tourbez, Y Blouquit, Microscopic viscosity and rotational diffusion of proteins in a macromolecular environment, Biophys J 76:2744-2751, 1999.

Kamyshny A, I Ermolina, S Magdassi, Y Feldman, Study of the dynamic structure of native and hydrophobized glucose oxidase by time-domain dielectric spectroscopy, J Phys Chem B 104:7588-7594, 2000.

Bonincontro A, A De Francesco, G Onori, Temperature-induced conformational changes of lysozyme in aqueous solution by dielectric spectroscopy, Chem Phys Letters 301:189-192, 1999.

Smith G, AP Duffy, J Shen, CJ Olliff, [Review Article] Dielectric relaxation spectroscopy and some applications in the pharmaceutical sciences, J Pharm Sci 84(9):1029-1044, 1995.

Buchner R, GT Hefter, PM May, Dielectric relaxation of NaCl solutions, J Phys Chem A 103(1):1-9, 1999.

Georgakilas AG, KS Haveles, EG Sideris, Dielectric study of the double helix to single coil transition of DNA, IEEE Trans Dielec Insul 5:26-32, 1998.

Nandi N, B Bagchi, [Letter] Anomalous dielectric relaxation of aqueous protein solutions (with supplementary materials/supporting info 18-26), J Phys Chem A 102(43): 8217-8221, 1998.

Nortemann K, J Hilland, U Kaatze, Dielectric properties of aqueous NaCl solutions at microwave frequencies, J Phys Chem A 101(37):6864-6869, 1997.

Lamm G, GR Pack, Local dielectric constants and Poisson-Boltzmann calculations of DNA counterion distributions, Int J Quant Chem 65:1087-1093, 1997.

Zakrzewska K, A Madami, R Lavery, Poisson-Boltzmann calculations for nucleic acids and nucleic acid complexes, J Chem Phys 204:263-269, 1996.

Duguid JG, VA Bloomfield, Electrostatic effects on the stability of condensed DNA in the presence of divalent cations, Biophys J 70:2838-2846, 1996.

Pack GR, GA Garrett, L Wong, G Lamm, The effect of a variable dielectric coefficient and finite ion size on Poisson-Boltzmann calculations of DNA electrolyte systems, Biophys J 65:1363-1370, 1993.

Bigio IJ, TR Gosnell, P Mukherjee, JD Safer, Microwave spectroscopy of DNA, Biopolymers 33(1):147-150, 1993.

Maleyev VY, MA Semenov, AI Gasan, VA Kashpur, Physical properties of the DNA-water system, Biophys 38:785-801, 1993.

Ruderman G, JR De Xammar Oro, On the dielectric spectra of proteins in conducting media, J Biolog Phys 18:167-174, 1992.

Saxena VK, LL Van Zandt, Effect on counterions on the spectrum of dissolved DNA polymers, Phys Rev A 45:7610-7620, 1992.

Saif B, RK Mohr, CJ MontroseTA Litovitz, On the mechanism of dielectric behavior in aqueous DNA solutions, Biopolymers 31(10):1171-1180, 1991.

Pedone F, A Bonincontro, Temperature dependence of DNA dielectric dispersion at radio frequency, Biochem Biophys Acta 1073:582-584, 1991.

Foster KR, BR Epstein, MA Gealt, “Resonances” in the dielectric absorption of DNA?, Biophys J 52(3):421-425, 1987.

Sakamoto M, R Hayakawa, Y Wada, Dielectric relaxation of DNA solutions, IV Effects of salts and dyes, Biopolymers 19:1039-1047, 1980.

Sakamoto M, R Hayakawa, Y Wada, Dielectric relaxation of DNA solutions, III Effects of DNA concentration, protein contamination, and mixed solvents, Biopolymers 18:2769-2782, 1979.

Sakamoto M, R Hayakawa, Y Wada, Dielectric relaxation of DNA solutions, II, Biopolymers 17:1507-1512, 1978.

Hanss M, JC Bernengo, Dielectric relaxation and orientation of DNA molecules, Biopolymers 12:2151-2159, 1973.

Takashima S, Dielectric dispersion of deoxyribonucleic acid, J Phys Chem 70(5):1372-1379, 1966.